Polar Science 19 (2019) 1–12

Contents lists available at ScienceDirect

Polar Science

journal homepage: www.elsevier.com/locate/polar

Greenland monthly precipitation analysis from the Arctic System Reanalysis (ASR): 2000–2012

Tomoko Koyama[a,b,c,*], Julienne Stroeve[d,a]

[a] National Snow and Ice Data Center, CIRES, University of Colorado Boulder, 449 UCB, Boulder, CO, 80309-0449, USA
[b] Department of Atmospheric and Oceanic Sciences, University of Colorado Boulder, 311 UCB, Boulder, CO, 80309-0311, USA
[c] Arctic Environment Research Center, National Institute of Polar Research, 10-3 Midori-cho, Tachikawa-shi, Tokyo, 190-8518, Japan
[d] Centre for Polar Observation and Modelling, Earth Sciences, University College London, Gower Street, London, WC1E6BT, UK

ARTICLE INFO

Keywords:
Arctic
Greenland
Precipitation
North atlantic oscillation

ABSTRACT

Arctic System Reanalysis version 1 (ASRv1) forecasts of monthly precipitation over Greenland are compared with gauge-based precipitation measured by the Danish Meteorological Institute (DMI) and precipitation retrieved from the Precipitation Occurrence Sensor System (POSS) at Summit. The ASRv1 precipitation generally agrees with the corrected DMI gauge-based precipitation measured at coastal or near-coastal stations in Greenland, but the corresponding data at Ikerasassuaq and Nuuk are not the case. ASRv1 precipitation at Summit, i.e., in a higher continental environment, is overestimated compared with the POSS observations. The North Atlantic Oscillation (NAO index and ASRv1 precipitation are moderately correlated over northern Greenland, the North Atlantic, and the Greenland Sea regions (0.32–0.49). It is presumed that local wind events have a larger influence on precipitation where smaller correlations occur. Suggested future work to understand discrepancies between ASRv1 and DMI precipitation fields in Greenland coastal regions is to include case studies of local wind events and corresponding precipitation variations utilizing in-situ measurements during both strong positive and negative NAO phases. At high-altitude and inland areas, further observations are needed to confirm the ASRv1 overestimation.

1. Introduction

The Greenland ice sheet (GrIS) has been losing mass in recent decades (1992–2011) at an estimated rate of 142 ± 49 Gt per year, with an increase in mass loss rate from 51 ± 65 Gt per year (1992–2000) to 263 ± 30 Gt per year (2005–2010) (Shepherd et al., 2012). Another estimate based on measurements by NASA's Gravity Recovery and Climate Experiment (GRACE) showed similar mass loss rate, 265 ± 25 Gt per year (2002–2015), corresponding to 0.72 mm per year average global sea level rise (Forsberg et al., 2017). This mass loss has been dominated by increased ice sheet melt, which in recent years has contributed more to GrIS mass loss than that from ice dynamics (Enderlin et al., 2014). While surface albedo primarily governs ice sheet surface mass balance (SMB) (Bougamont et al., 2005; Tedesco et al., 2011; Box et al., 2012; Fitzgerald et al., 2012), summer snowfall events can counterbalance the positive melt-albedo feedback (Stroeve, 2001), by covering dark ice and/or metamorphosed snow with a highly reflective fresh snow layer (Noël et al., 2015).

At the same time, large reductions in Arctic sea ice extent (SIE) have occurred (e.g., Stroeve et al., 2012a; Serreze and Stroeve, 2015), leading to strong solar heating of the upper ocean. Increased ocean mixed layer heat content during summer results in large exchanges of heat and moisture during autumn and winter as the ice reforms. Enhanced heat and moisture fluxes from the ocean to the atmosphere are one of the drivers behind increased moisture content of the Arctic atmosphere (Serreze et al., 2012) as well as Arctic Amplification (AA), the outsized warming of the Arctic compared to the Northern Hemisphere or the global average (Serreze et al., 2009; Screen and Simmonds, 2010). Increased moisture content of the Arctic atmosphere may, in turn, be responsible for increased autumn and winter precipitation over Siberia (Cohen et al., 2012; Ghatak et al., 2012; Orsolini et al., 2013) as well as increases in Arctic snowfall extremes (Liu et al., 2012; Bintanja and Selten, 2014). The impact of sea ice loss on Greenland accumulation, however, remains less clear.

Expanding open water areas, however, do appear to be in part responsible for locally sourced moisture that could impact precipitation over Greenland. Kopec et al. (2016) found an increase of the proportion of moisture sourced from the Arctic concerning sea ice reductions in the

* Corresponding author. Arctic Environment Research Center, National Institute of Polar Research, 10-3 Midori-cho, Tachikawa-shi, Tokyo, 190-8518, Japan.
E-mail addresses: koyama.tomoko@nipr.ac.jp (T. Koyama), stroeve@nsidc.org (J. Stroeve).

https://doi.org/10.1016/j.polar.2018.09.001
Received 11 April 2018; Received in revised form 29 August 2018; Accepted 7 September 2018
Available online 14 September 2018

Canadian Arctic and Greenland Sea regions over the past two decades. However, precipitation observations do not show a significantly increasing trend with respect to sea ice loss in these two regions. On the other hand, several studies have examined how Arctic warming and associated changes in turbulent fluxes may impact cyclone activity in the Arctic (McCabe et al., 2001; Yin, 2005; Bengtsson et al. 2006, 2009; Ulbrich et al., 2009; Inoue et al., 2012; Akperov et al., 2015; Koyama et al., 2017). Some regional features have emerged, such as a northward shift in cyclones tracking through the North Atlantic (Zhang et al., 2004; Yin, 2005; Ulbrich et al., 2009; Koyama et al., 2017) with the potential to impact GrIS precipitation. Koyama et al. (2017) showed an increased potential for cyclogenesis around Greenland during low sea ice years. The combination of more moisture availability and increased cyclogenesis, may further increase the intensity of cyclones, and increase the amount of cyclone-associated precipitation, leading to increased snowfall.

While the quantitative link between precipitation and SIE remains poorly constrained, Appenzeller et al. (1998) found a linear relationship between snow accumulation and the North Atlantic Oscillation (NAO) (Hurrell, 1995) index in western central Greenland. The NAO describes a tendency toward simultaneous strengthening or weakening of the subpolar (Icelandic) Low and the subtropical (Azores) High, impacting general climate conditions for the North Atlantic Ocean basin and the strength of meridional transport (Koerner and Russell, 1979). Bromwich et al. (1999) utilized an indirect dynamic approach over Greenland and estimated the precipitation from wind, geopotential height, and moisture fields. While this approach can be referred to Chen et al. (1997), the ω equation method based on an equivalent isobaric geopotential height in σ coordinates allows a vertical motion computation over high mountain regions. By computing the advection and adiabatic variations of the temperature and specific humidity, excess water through a layer can be obtained by removing supersaturation from the specific humidity field. Subsequently, falling water, saturation, and evaporation through multiple layers are computed. The precipitation and latent heat release can be derived in the end. The results showed that increased precipitation in southern Greenland occurs with variations in the position and intensity of the Icelandic Low, which is related to the NAO. Mosley-Thompson et al. (2005) documented that the NAO influence on Greenland precipitation weakens along the west-central side of the ice sheet and strengthens in the southeastern region when the temperature rises. Box et al. (2012) discussed on strong anticyclonic circulation centered over Greenland that associated with a persistent negative summer NAO index in 2000–2011. Such conditions enhance warm air advection along the western ice sheet and reduce cloudiness and summer snowfall precipitation. These are amplifying mechanisms to maximize the albedo feedback. Fettweis et al. (2013) showed that anticyclonic conditions over Greenland gauged by negative NAO indexes were increased. Hanna et al. (2014) studied record surface melting of the GrIS in July 2012 and showed that a blocking high pressure feature in the mid-troposphere over Greenland for the summer was associated with negative NAO conditions. Sea surface temperature and sea-ice cover anomalies seem to have played a minimal role during this period.

As the sea ice is simulated to continue to decline through the end of the twenty-first century (e.g., Stroeve et al., 2012b; Massonnett et al., 2012; Stroeve and Notz, 2015; Jahn et al., 2016; Notz and Stroeve, 2016), precipitation over the Arctic Ocean is projected to increase (Kattsov et al., 2007; Bintanja and Selten, 2014), with the potential to increase the GrIS SMB if the precipitation falls as snow. When the precipitation falls as rain, only the part of rainfall that refreezes can contribute to mass gain, and it decreases surface albedo which enhances surface melt (Vizcaíno et al., 2014). On the other hand, Lim et al. (2016) found that the negative phase of the NAO is associated with warm and dry conditions for the GrIS, leading to SMB decreases. Thus, it is important to understand better how precipitation has and may change in the future, as a warmer troposphere is more likely to produce rainfall rather than snowfall. Unfortunately, such an assessment has not been attainable due to the lack of observations. Observations of Greenland precipitation are limited, and the ones that exist (e.g., gauge measurements) suffer from wind effects contamination and are generally confined to the coastal regions.

The lack of reliable and accurate observations of precipitation has led to many studies using atmospheric reanalysis data to evaluate changing Arctic precipitation (Serreze et al., 2015; Kopec et al., 2016). Atmospheric reanalyses are retrospective forms of numerical weather forecasts that assimilate observational data into a short-term forecast model using the observations as a first guess of the state of the atmosphere. Recently, an Arctic-focused reanalysis product was developed to specifically assess and monitor variability and change over the greater Arctic region under a U.S. program, the Study of Environmental Arctic Change (SEARCH). The Arctic System Reanalysis (ASR) (Bromwich et al., 2010) was developed as a synthesis tool for assessing and monitoring variability and change in the Arctic system. Bromwich et al. (2016) compared the ASR forecast monthly precipitation totals with gauge observations on land from the Global Historical Climate Network version 2 (GHCN2) (Peterson and Vose, 1997) and the Adjusted Historical Canadian Climate Data (AHCCD) (Mekis and Hogg, 1999) within the ASR domain, including Greenland, for the period December 2006 to November 2007. While they showed that the ASR precipitation is generally less (more) during cool (warm) months than observed, the comparison was performed for a limited time, over 12 months. They also compared the monthly total precipitation for the ASRv1 and the European Center for Medium-Range Weather Forecasts (ECMWF) Interim Re-Analysis (ERA-Interim) (Dee et al., 2011). However, the comparison was performed where the GHCN2 and AHCCD gauges are located at for the period December 2006–November 2007. Thus, they utilized a small set of over-land locations' data, and the results did not include the spatial distribution over Greenland and the surrounding waters.

This study aims to assess the accuracy of the ASR precipitation fields along the coastal region of Greenland for the entire ASR time-period (2000–2012) through comparisons with ground-based station data and X-band Doppler radar measurements at Summit. The results of our study complement the findings of Bromwich et al. (2016) by utilizing different observations over a different study period and a different region. Additionally, we explore the relationship between the NAO index and ASR precipitation over Greenland.

2. Datasets and methodology

Two datasets are used to evaluate the ASR version 1 (ASRV1) precipitation data around Greenland: gauge-based precipitation measured by the Danish Meteorological Institute (DMI) (Cappelen, 2014); and precipitation retrieval from the Precipitation Occurrence Sensor System (POSS), which is a bistatic, continuous-wave, X-band Doppler radar utilized in the Integrated Characterization of Energy, Clouds, Atmospheric state and Precipitation at Summit (ICECAPS) project (Sheppard and Joe, 2008; Castellani et al., 2015). The first dataset, ASRv1, spans 2000–2012 and the spatial coverage extends beyond the boundaries of the Arctic Ocean. The spatial resolution of ASRv1 is 30 km, and the temporal resolution is 3-hourly. Among six produced ASRv1 datasets for users, variables designated as “accumulated total grid scale precipitation” and “accumulated total cumulus precipitation” stored in the “ASR Final 30 km 2D surface forecast product” are utilized to derive total precipitation since they are non-convective and convective precipitation, respectively. The accumulated amount of this total precipitation over a month is defined as the ASRv1 monthly precipitation in this study. Note that cumulus convection is not accurately represented in numerical models and excessive precipitation tends to be produced (Fonseca et al., 2015). Bromwich et al. (2016) reported that convective precipitation over land in summer is excessive, but the issue is resolved in version 2 (ASRv2). ASRv2 also has improved the spatial

Table 1
Information about the selected DMI stations and POSS.

Station ID	Location	Monthly data numbers	Latitude	Longitude	Elevation (a.s.l.)
04310	Station Nord	58	81.6°N	16.7°W	36 m
04320	Danmarkshavn	71	76.8°N	18.7°W	11 m
04339	Ittoqqortoormiit	108	70.5°N	22.0°W	65 m
04360	Tasiilaq	142	65.0°N	37.6°W	53 m
04390	Ikerasassuaq	127	60.0°N	43.2°W	26 m
04270	Mitt. Narsarsuaq	105	61.2°N	45.4°W	27 m
04272	Qaqortoq	150	60.7°N	46.1°W	32 m
04250	Nuuk	110	64.2°N	51.8°W	54 m
04231	Kangerlussuaq	111	67.0°N	50.8°W	50 m
04220	Aasiaat	111	68.7°N	52.8°W	43 m
POSS	Summit	27	72.6°N	38.5°W	3260 m

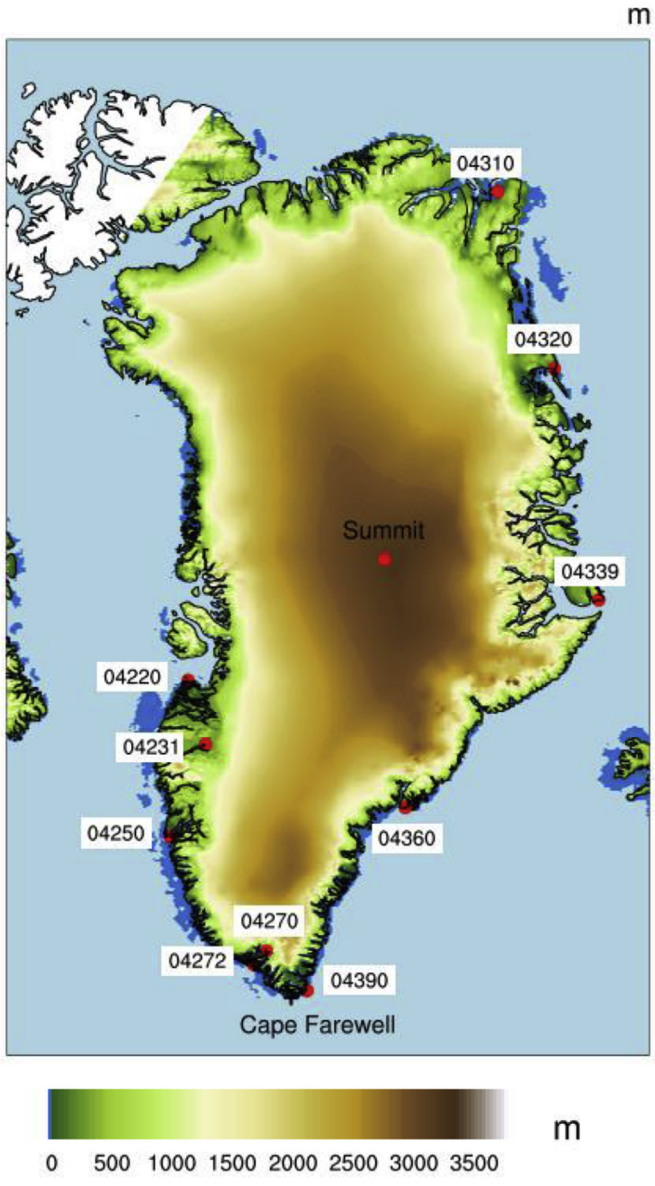

Fig. 1. DMI stations used for this study and Summit where the POSS is located.

resolution of 15 km, and while fields of precipitation and radiation are expected to be improved, ASRv2 was not available in time for this study.

The second dataset is the DMI historical data collection 1873–2012

Table 2
Correlation coefficients between the ASRv1 precipitation and the DMI/POSS precipitation. All values are statistically significant ($p \leq 0.05$).

Station ID	1 × 1 patch	3 × 3 patch	5 × 5 patch
04310	0.83	0.80	0.75
04320	0.78	0.77	0.75
04339	0.81	0.82	0.82
04360	0.80	0.82	0.82
04390	0.59	0.59	0.57
04270	0.84	0.83	0.80
04272	0.85	0.86	0.84
04250	0.37	0.38	0.40
04231	0.66	0.67	0.62
04220	0.70	0.72	0.76
POSS	0.57	0.54	0.50

Table 3
Mean values of monthly precipitation of DMI (POSS) and the corresponding ASRv1 values from the three different coverage size.

Station	DMI (POSS) [mm]	ASR 1 × 1 [mm]	ASR 3 × 3 [mm]	ASR 5 × 5 [mm]
04310	23.1	40.5	35.3	30.7
04320	14.9	23.8	24.0	25.1
04339	36.3	54.8	54.9	58.6
04360	67.0	84.6	90.6	99.8
04390	138.3	166.9	154.0	143.4
04270	50.1	85.9	100.9	118.4
04272	73.6	76.4	81.6	94.7
04250	84.3	54.0	60.8	66.5
04231	14.9	21.5	24.3	31.4
04220	26.9	32.1	32.5	33.4
POSS	5.5	13.6	13.7	14.1

for Greenland. Eighty-eight DMI weather stations are located in coastal or near-coastal (less than 100 m a.s.l.) regions. Comprehensive quality control was applied to the whole dataset, and erroneous data were removed. Measurement periods of the DMI gauges vary significantly among these stations resulting in many stations lacking data during our study period. DMI stations where numbers of observations reached more than a third of the study period of the data available from the ASRv1 (156 months of data from 2000 to 2012) are selected for comparison, i.e., stations having at least 52 monthly observations during the 13 years. This selection was aimed to secure a reasonable degree of confidence and resulted in only ten stations being identified for comparison with the ASRv1 precipitation. Also, the observed data quality among stations may vary due to differences in the automated observation system and frequencies of maintenance and calibration (Cappelen, 2014). Table 1 and Fig. 1 show the locations of those selected stations including the Summit POSS (described below). To derive 24 h accumulated precipitation, considering wind-induced undercatch, wetting loss, and trace precipitation amounts, a precipitation bias is corrected following Yang et al. (1999):

$$P_c = \frac{CR}{100}(P_g + \Delta P_w + \Delta P_e) + \Delta P_t$$

where P_C, P_g, ΔP_w, ΔP_e, and ΔP_t in millimeters are corrected precipitation, gauge-measured precipitation, wetting loss, evaporation loss, and trace precipitation, respectively. ΔP_w, i.e., wetting loss, is varied by precipitation type and the number of times the gauge is emptied. ΔP_e, i.e., evaporation loss, depends on gauge type and time of the year. ΔP_t, i.e., trace precipitation, is generally an unmeasurable quantity of precipitation, but inversely proportional to the gauge-measured annual precipitation and this correction is important in northern Greenland (Yang et al., 1999). Daily catch ratio (CR in %) is a function of daily wind speed and three precipitation types: snow, rain, and mixed precipitation. Although precipitation types were unknown at

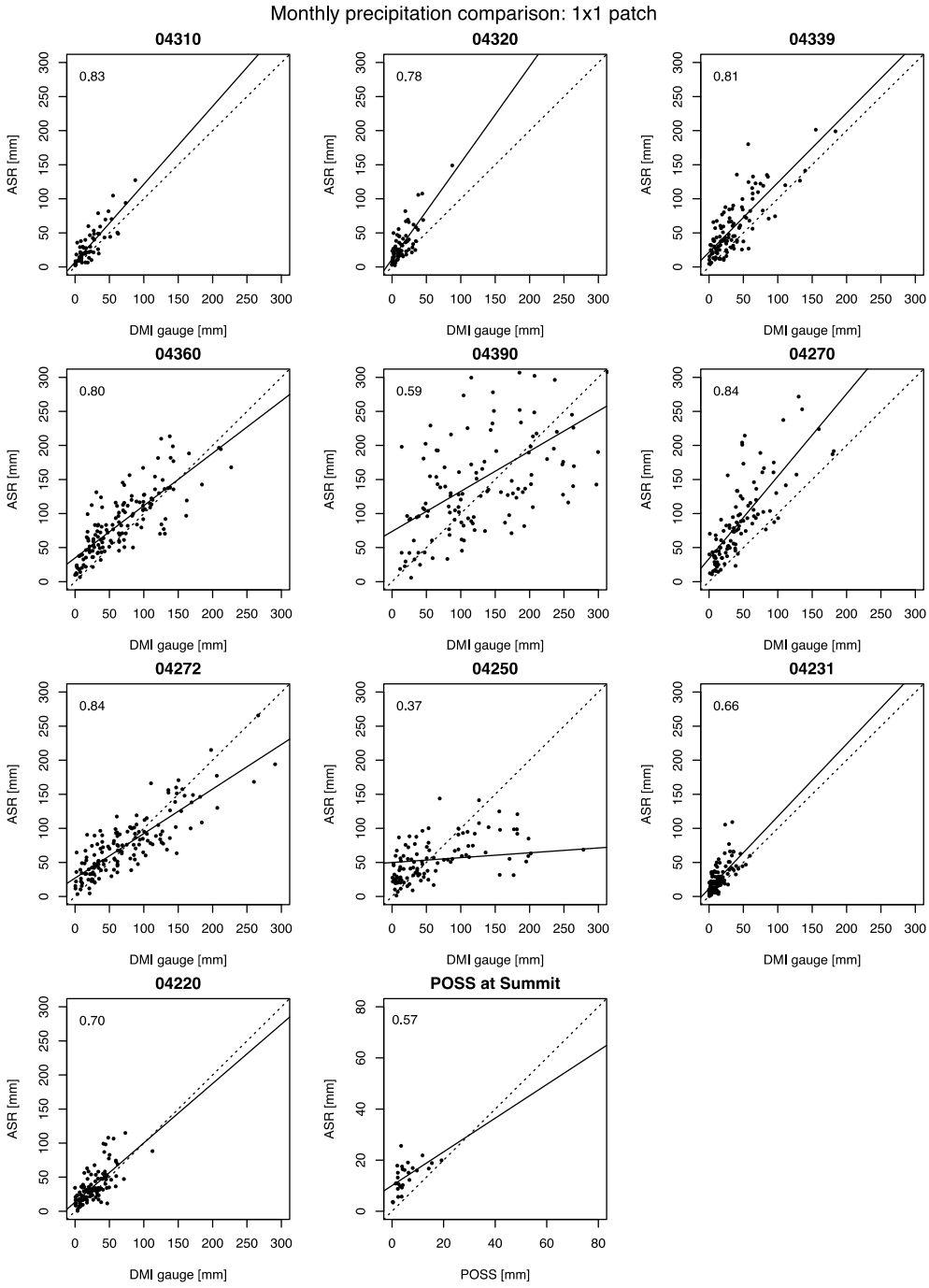

Fig. 2. Scatterplot of the ASRv1 1x1-patch monthly precipitation and the DMI/POSS monthly precipitation and numbers at top right corners show the correlation coefficients. Solid lines indicate linear regressions. Statistical significance of the correlation can be found in Table 2.

the selected stations, a simple assumption based on the near-surface air temperature was made to determine the type of precipitation. If all the observations in a single day indicate below (above) zero Celsius, i.e., freezing point, the daily precipitation type is snow (rain), and otherwise, it is mixed precipitation. The monthly DMI precipitation used for the comparison is represented as the accumulations of those daily corrected precipitation data, which is based on the reported 24-h accumulated precipitation (Cappelen, 2014).

The third dataset is from the POSS located at Summit, one of the highest elevation locations within the Arctic, and is used to assess ASRv1 precipitation within the interior of the ice sheet. POSS operated from September 2010 to present, resulting in 27 months of snowfall data that overlap with the ASRv1 dataset. Snowfall retrieval from POSS is based on the so-called Z-S relationship between the equivalent reflectivity factor and water equivalent (w.e.) snowfall rate using the T-matrix scattering model (Mishchenko, 2000). The Z-S relationship is expressed as $Z = BS^{\beta}$, where Z is the equivalent reflectivity factor or reflectivity, S is snowfall rate, and B and β are coefficients. These coefficients depend on crystal habits and the snow size distribution, which are not observed, leading to a certain level of uncertainty in the POSS snowfall rate. Associated with the time-space comparison, the effective uncertainty of POSS reflectivity is likely to be within 3 dB, which is equivalent to a factor two uncertainty in snowfall (Castellani et al., 2015). Consequently, the POSS monthly precipitation used for the comparison consists of this daily precipitation accumulated over a month. Further information about POSS and/or radar-based snowfall

Table 4
Linear regression constants and accuracy measures between the ASRv1 precipitation and the DMI/POSS precipitation.

Station ID	Intercept [mm]	Slope	Bias [mm]	Root Mean Square Error [mm]
04310	7.0	1.1	10.3	18.2
04320	11.4	1.4	17.5	24.7
04339	21.6	1.0	22.3	33.3
04360	34.7	0.8	19.3	35.7
04390	73.8	0.6	17.0	81.2
04270	33.8	1.21	44.3	58.8
04272	27.0	0.7	1.5	31.1
04250	49.9	0.1	−28.4	161.7
04231	11.3	1.1	12.3	19.4
04220	13.2	0.9	9.7	19.8
POSS	10.0	0.7	8.2	9.5

retrievals can be found in Matrosov (2007), Matrosov et al. (2009), Sheppard and Joe (2008), and Castellani et al. (2015).

The nearest ASRv1 grid point to each DMI station or the POSS location was initially selected for comparison. Recalling that precipitation depends on subgrid-scale physical processes, we do not know whether precipitation amount at the nearest ASRv1 grid point represents that at the corresponding station with acceptable uncertainty. To find an adequate area to represent each measurement location, three patches of various sizes (1 × 1, 3 × 3, and 5 × 5 grid points) are defined. While a 1 × 1 patch is equal to the nearest grid point to the measurement site, 3 × 3 and 5 × 5 patches are the areas having the nearest grid points in the center. Consequently, monthly ASR 1x1-patch precipitation is the same as the ASRv1 monthly precipitation at the nearest point to the measurement site, and the corresponding spatial mean values are defined as 3x3-and 5x5-patch monthly precipitation. The Pearson's correlation coefficient between the ASRv1 monthly precipitation and the DMI (POSS) monthly precipitation is computed to measure the linear correlation. The seasonal and interannual variability of the DMI, ASRv1, and POSS monthly precipitation are visually examined at each site.

The NAO index data used in this study is obtained from the National Oceanic and Atmospheric Administration (NOAA) Climate Prediction Center (CPC; www.cpc.ncep.noaa.gov/products/precip/CWlink/pna/nao.shtml). The monthly NAO index is defined as a principal component of the Atlantic centered rotated empirical orthogonal function analysis of the monthly mean 500-mb height north of 20°N. Further information can be found on the CPC website.

3. Results

3.1. Comparison of monthly precipitation

Table 2 lists the correlation coefficients between the DMI (POSS) precipitation and the ASRv1 precipitation obtained from the three different coverage sizes described in the previous section. These correlations are all statistically significant at $p \leq 0.05$. Overall, they are positively correlated, and the range is from 0.37 to 0.86, indicating that temporal representativeness of the ASRv1 precipitation varies strongly by location. While the ASRv1 1x1-patch and the DMI precipitation have larger correlations in the south and northeast of Greenland, correlation coefficients with respect to the 5x5-patch are larger than those with respect to the 1x1-or 3x3-patches in eastern and western Greenland. However, correlation coefficients for the 3 × 3 and 5 × 5 patches generally only differ by ± 0.04, suggesting precipitation at the nearest ASRv1 grid point is representative of the corresponding DMI station. Table 3 summarizes the mean values of monthly precipitation from DMI (POSS) and the corresponding ASRv1 values derived from the three different coverage sizes. In general, the ASRv1 1x1-patch values show the best agreement with the DMI (POSS) values, further confirming the nearest ASRv1 grid point is sufficient to represent the corresponding DMI station. The following figures only show results for the 1 × 1 patch.

Fig. 2 shows the ASRv1 1x1-patch precipitation against the DMI (POSS) precipitation at each station location. Table 4 lists the corresponding linear regression coefficients, and the bias and root mean square errors (rmse). In general, precipitation at the DMI stations located on the east side of Greenland (04310, 04320, 04339, 04360, 04270, and 04272) show the best agreement with the corresponding ASRv1 precipitation, with correlation coefficients in the range of 0.75–0.86. ASRv1 precipitation at three northeastern stations, 04310, 04320, 04339, and a southern station 04270 exhibit apparent positive biases that are not dependent on precipitation amount received. On the other hand, ASRv1 precipitation at stations 04360 and 04272 show positive biases during light precipitation periods and negative biases when the monthly precipitation amount exceeded 150 mm. While moderate correlations (0.57–0.76) appear at stations 04390, 04231, and 04220, station 04250 (Nuuk) shows the lowest correlation (0.37) among all the DMI stations. Nuuk receives about 100 mm per month of precipitation (Aðalgeirsdóttir et al., 2009), and the majority of the corresponding ASRv1 data show a negative bias.

It is known that there are challenges in measuring solid precipitation, such as blockage of the gauge orifice by snow capping the gauge; accumulation on the side of the orifice walls; wind undercatch of snow due to the formation of updrafts over the gauge orifice; the unknown role of turbulence on gauge catch; and the large variability in gauge catch efficiency for a given gauge and wind speed (Rasmussen et al., 2012). Thus, the wind field around the gauge can significantly affect the quality and accuracy of precipitation data. While gale-force winds frequently occur in Southern Greenland from westerly or easterly tip jets, northeasterly barrier winds, or northwesterly katabatic winds (Moore et al., 2016), topography-induced airflow can also influence local precipitation. The effects of area-specific variability in winds are less likely to be reflected in the coarse resolution ASRv1 precipitation estimates where the terrain is complex. For example, Nuuk at the mouth of Nuup Kangerlua is part of the large Nuuk fjord system, and the smoother topography used in the model can cause high bias in surface wind forecast there. Moore et al. (2016) documented that a horizontal grid size on the order of 15 km is needed to characterize the impact that Greenland's topography has on the regional wind field and climate. Station 04390 (Ikerasassuaq) shows a large scatter between the station data and ASRv1, and this too may also be a result of topographic effects. Moore and Renfrew (2005) studied surface winds over Southern Greenland from December to February using Quick Scatterometer (Quick-SCAT) data and found highly localized maxima wind speeds just to the south and east of Cape Farewell, which is near Ikerasassuaq. It is plausible that the ASRv1 forecast precipitation error is likely to be larger when the stronger wind is observed.

Fig. 3 shows the time series of the ASRv1 1x1-patch and DMI precipitation at the target DMI stations, respectively. The blue line shows local polynomial regression fitting, and the light blue shading shows the 95% confidence intervals. The month-to-month variability at each station is large as well as the rmse values in Table 4 display. Thus, it is difficult to detect seasonal variability from the monthly data over 13 years. Consequently, the majority of the ASRv1 precipitation values are outside of the 95% confidence intervals and the following discussion is based on the regression curves. Interannual variability at stations 04270 and 04272 are similar to each other as they are located in the vicinity in the southern coast of Greenland (Fig. 3a). Gradual precipitation increase (decrease) is observed from 2000 to 2004 (2006–2008) at the two stations. Trends at stations 04310 and 04320 located on the northeastern coast of Greenland are also similar to each other. Local maximum values appear in 2006 at both stations, which are reflections of the extremely large observed values (Fig. 3a). Similar to the ASRv1 precipitation trends, the majority of the DMI precipitation values are outside of the 95% confidence intervals of the local polynomial regression fitting (Fig. 3b). It is not appropriate to discuss the

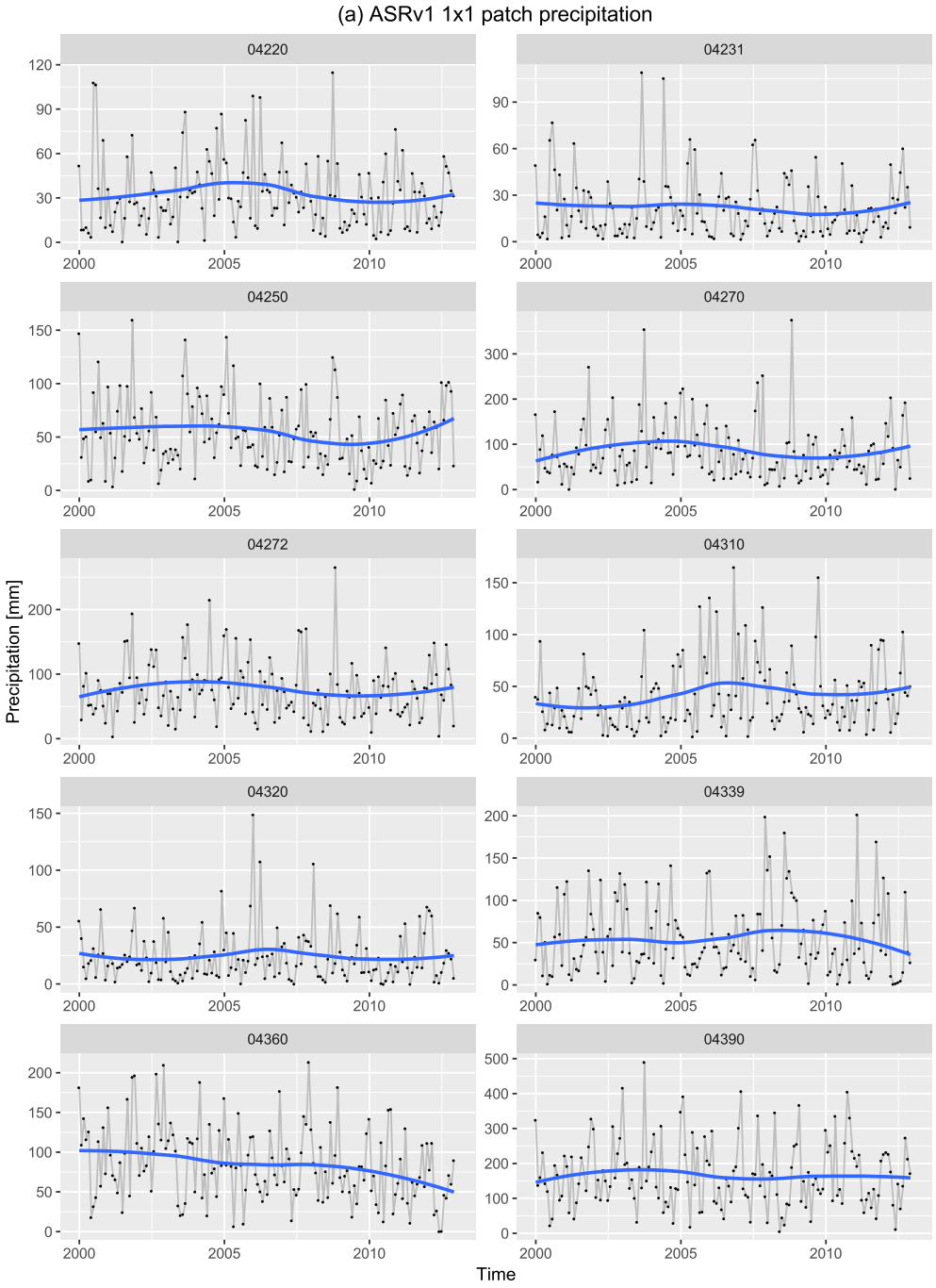

Fig. 3. (a) time series of the ASRv1 1x1-patch monthly precipitation at the DMI stations and (b) corresponding DMI precipitation. Each graph is plotted in the optimized range for precipitation (y-axis) at the corresponding location. The blue line shows local polynomial regression fitting, and the light blue shading shows the 95% confidence intervals.

trends from the available DMI data since some stations have discontinuous observations in addition to the sample size limitations, but the stations 04220, 04231, 04272, and 04390 show increasing trend at the end of the study period. The lowest Arctic sea ice extent during the satellite era was recorded in this year. The station 04250 trend looks unique since it shows an extreme precipitation amount (over 1500 mm per month). However, it is reasonable to assume this extreme value is an erroneous observation. Maximum values of the time series at other locations such as the stations 04220, 04270, and 04320 also might be erroneous. While DMI claimed the data series in question, not all have been tested for homogeneity nor homogenized (Cappelen, 2014), we had not performed additional quality control to maintain the sample size. In-situ precipitation measurements are supposed to be the most reliable data even if uncertainty due to undercatch occurs. Since steadily accurate measurement in the Arctic has been unattainable due to the harsh environment, a sustained effort must be made for improved hydrometeorological analyses.

Fig. 4 shows the time series of precipitation at Summit, the POSS and ASRv1 1x1-patch precipitation. As we see in Fig. 2, the ASRv1 precipitation is larger than the retrieved POSS precipitation and the trend lines for the two datasets do not agree. However, the period of available monthly precipitation data (a little over two years) is not sufficient time to adequately identify interannual variability at Summit.

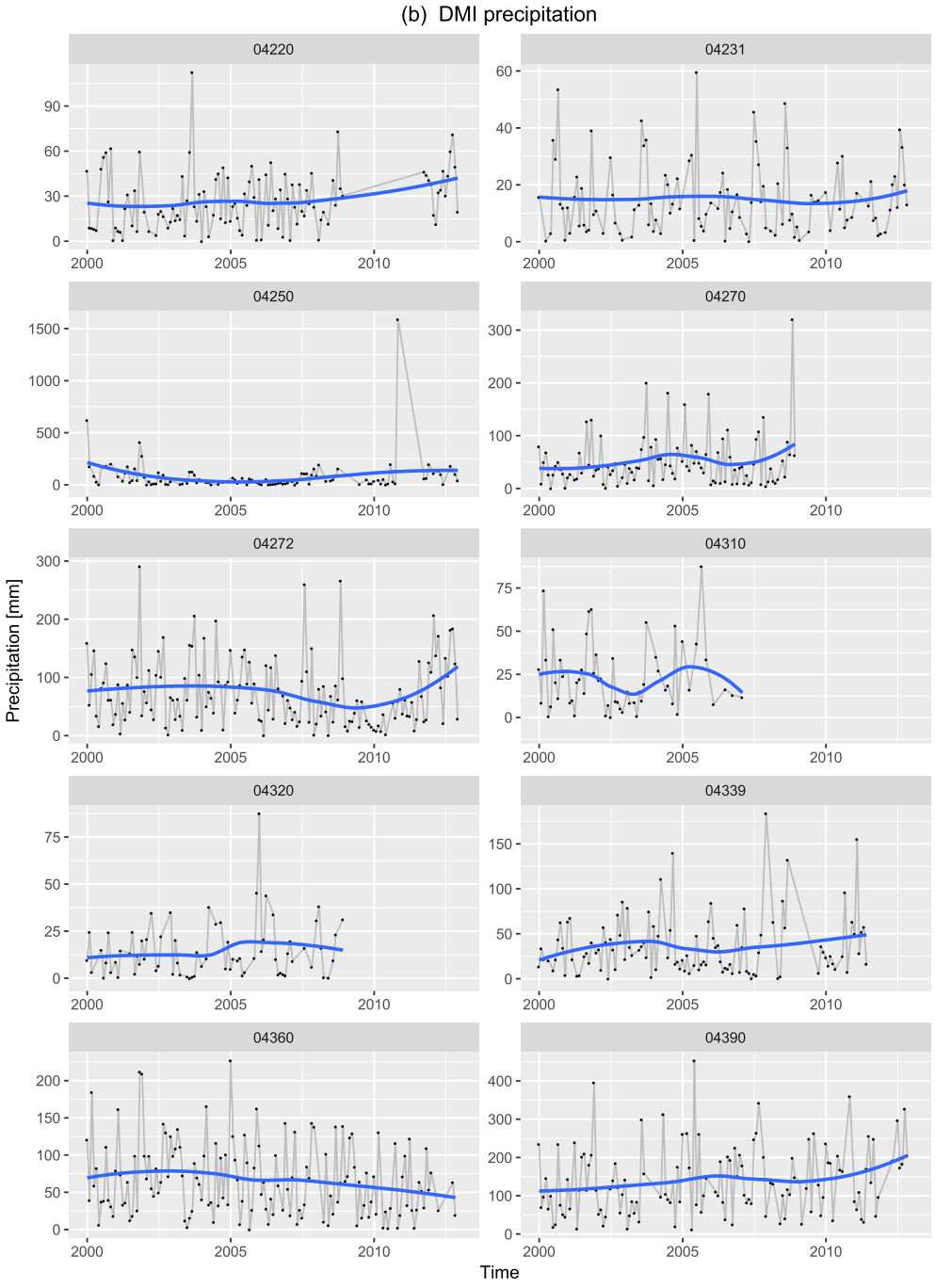

Fig. 3. (*continued*)

3.2. The Northern Atlantic oscillation (NAO) and precipitation

The spatial distribution of precipitation is governed by atmospheric circulation, proximity to large bodies of water, and topography. Thus, it is better to divide Greenland and surrounding waters into regions with similar characteristics to study the relationship between local precipitation and the NAO index. Greenland is divided into four regions, based on the major ice sheet topographical divides following Stroeve et al. (2017): Northwest (NW), Southwest (SW), Southeast (SE), and Northeast (NE). Also, the surrounding waters, i.e., the Baffin Bay (BB), Davis Strait (DS), North Atlantic (NA), Greenland Sea (GS), Lincoln Sea (LS), Arctic Basin (AB), are defined as shown in Fig. 5. Note that the entire AB is not depicted in the figure due to the map projection (the Lambert conformal conic). The defined AB is approximately bordered by the continental shelves of Eurasia and North America.

Fig. 6 shows the relationship between the area averaged monthly ASRv1 precipitation over the divided regions and the corresponding monthly NAO index. The spatially averaged precipitation is derived from monthly ASRv1 precipitation at all available grid points in the region. The data period is from 2000 to 2012, and all 12 months of data are utilized as well as the monthly precipitation analysis. Correlation coefficients for the NW, SW, NE, and SE regions are −0.36, 0.09, 0.32, and 0.25, respectively. These values are statistically significant ($p \leq 0.05$) except for the SW (p-value of 0.24). Fig. 7 shows the relationship between the regionally averaged ASRv1 precipitation over surrounding waters, the BB, NA, GS, and AB regions, and the NAO index, in which the correlation coefficients are −0.27, 0.49, 0.46, and −0.14, respectively. The correlation coefficients are statistically significant ($p \leq 0.05$) for the BB, NA, and GS regions. The corresponding scatter plots for the LS and DS regions are not shown here, but their

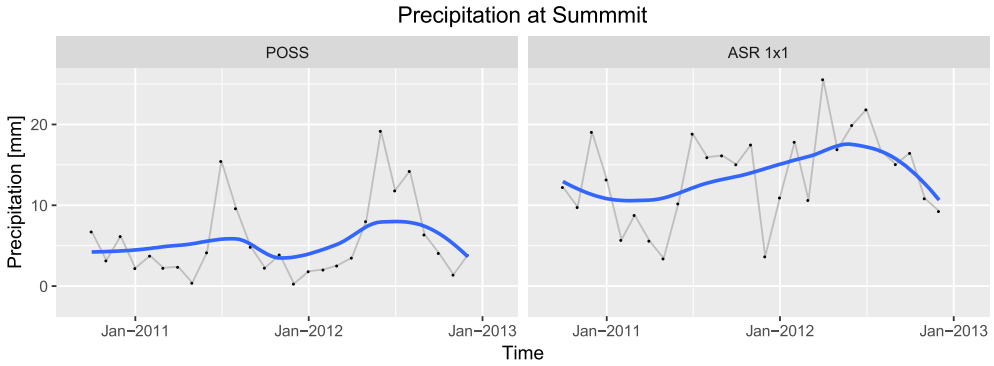

Fig. 4. Time series of the POSS and ASRv1 1x1-patch monthly precipitation at the corresponding location. The blue line shows local polynomial regression fitting, and the gray shading shows the 95% confidence intervals.

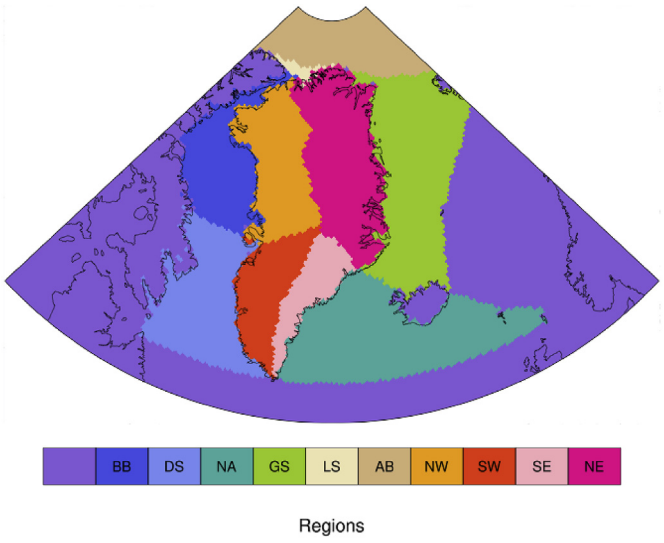

Fig. 5. Map of Greenland regions and surrounding waters, comprising Northwest (NW), Southwest (SW), Southeast (SE), Northeast (NE), the Baffin Bay (BB), the Davis Strait (DS), the North Atlantic (NA), the Greenland Sea (GS), the Lincoln Sea (LS), and the Arctic Basin (AB).

correlation coefficients are 0.01 and 0.11, respectively. Since the NAO is strongest and its most climatologically effective expression occurs during the cold season months (Rogers, 1984; Hurrell, 1995; Jones et al., 1997), the same analysis during the colder months (September–April) is performed. The colder months' correlation coefficients for the NW, SW, SE, SW, BB, DS, NA, GS, LS, and AB are −0.42, −0.01, 0.09, 0.39, −0.32, −0.01, 0.50, 0.48, 0.10, and −0.14, respectively. Among these values, the results for the NW, NE, BB, NA, and GS are statistically significant ($p \leq 0.05$), and their magnitudes are larger than the corresponding coefficients derived from the entire period except for the GS.

4. Discussion

In the Arctic, precipitation arrives as snow during nearly nine months out of the year, and sublimation directly returns moisture to the atmosphere (Liston and Sturm, 2004). Given that strong and frequent winds prevent us from measuring accurate precipitation, it is extremely challenging to observe precipitation at any place in the Arctic. Therefore, it is beneficial to understand the characteristics of the newly developed ASRv1 precipitation data for Arctic climate research. Arctic sea ice decline has increased the heat flux from the ocean to the atmosphere in autumn and early winter (Vihma, 2014). Consequently, sea ice loss is strongly tied to increased tropospheric moisture, precipitation and cloud cover (e.g., Francis et al., 2009; Kay and Gettelman, 2009; Screen et al., 2013; Abe et al., 2016; Vazquez et al., 2017). Regarding the GrIS SMB, changes in accumulation, mostly driven by precipitation, may help to counter ice mass loss from increased ice melt. Mernild et al. (2015) investigated coastal annual precipitation trends and showed positive (negative) trends in western (southern and eastern) Greenland over the 1991–2012 period. Similarly, Wong et al. (2015) showed positive annual precipitation trends at Thule air base in northwestern Greenland over the 1981–2012 period. While their results were based on gauge observations, mean precipitation in the interior of the GrIS was estimated from snow pits and ice cores in both studies and negligible changes in precipitation in the GrIS interior were found.

Note that uncertainty of observed precipitation in the Arctic tends to be larger than that in the lower latitude. Serreze and Barry (2014) provided major issues regarding measurement of precipitation: significant gauge undercatch of solid precipitation, the sparse station network, and large biases in precipitation estimates based on satellite observations or from atmospheric reanalyses. We can also assume that spatial and temporal patterns of precipitation are linked to moisture circulation caused by multi-scale dynamics. Thus, it is difficult to reach a solid understanding of ASRv1 precipitation utilizing a few sets of analyses. Future comprehensive work will entail a further understanding of precipitation in the Arctic. For example, precipitation data from regional climate models forced by reanalysis datasets (e.g., Noël et al., 2015; Fettweis et al., 2017; Langen et al., 2017; Niwano et al., 2018) are worthy to access the reliability to cover insufficient in-situ observations in the Arctic.

Our results show good agreement between the gauge and ASRv1 precipitation data at coastal locations except for stations at Ikerasassuaq and Nuuk. Nevertheless, there is a significant discrepancy between the ASRv1 precipitation and retrieved POSS precipitation at Summit, as well as their trends (Figs. 2 and 4). The ASR monthly precipitation is always larger than the corresponding POSS retrievals (Fig. 4). The correlation coefficient is about 0.5 and the rmse is 9.47 mm as shown in Tables 2 and 4, respectively. As for the estimated POSS precipitation, the annual values for 2011 and 2012 are 51.8 and 79.1 mm water equivalent (w.e.), respectively. Assuming the reflectivity uncertainty is a factor of two, the maximum limits of the estimations are 103.6 and 158.2 mm w.e. for 2011 and 2012, respectively. These uncertainties are inevitable due to the inherent indirect nature of radar observations. According to observations by Castellani et al. (2015), the mean annual POSS snowfall based on measurements from September 2010 to October 2013 was 92.5 mm w.e. with a potential spread between 81.1 and 126.7 mm w.e. due to uncertainty in the assumed undercatch ratio. On the other hand, the ASRv1 annual precipitation at Summit is 134.3 and 192.2 mm w.e. for 2011 and 2012, respectively. Therefore, the estimated POSS precipitation amounts are still smaller than the ASRv1 estimate at Summit. This result is not conclusive since the comparison is over only 27 months and the p-value

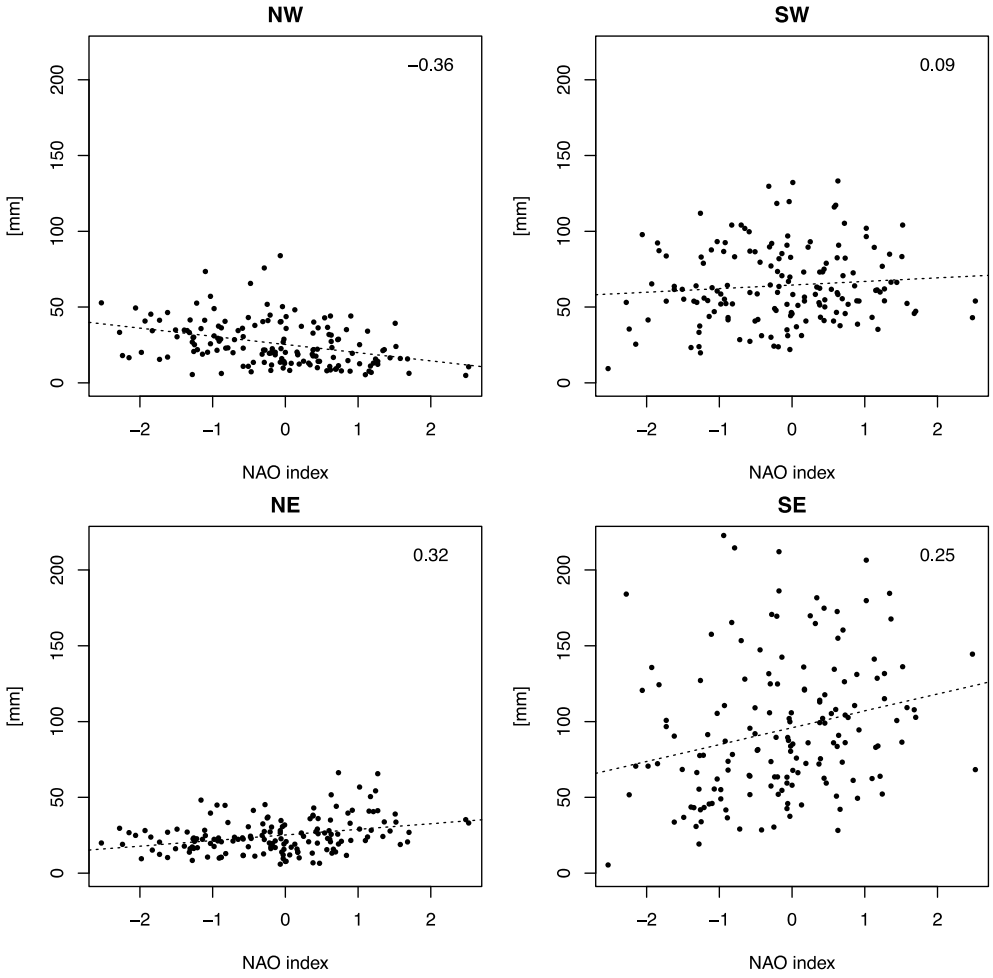

Fig. 6. Area-averaged monthly ASRv1 precipitation and the NAO index over four regions in Greenland. Dotted lines indicate linear regressions and numbers at top right corners show the correlate coefficients.

is 0.30. In fact, other estimations of the annual precipitation based on a pit or regional climate modeling studies are in the range of 170–200 mm w.e. in the area near Summit (Bales et al., 2001; Ettema et al., 2009). Berkelhammer et al. (2016) discussed that little to no net water vapor exchange occurs at the surface at Summit in winter, and the hydrological budget in summer is controlled by condensation, sublimation/evaporation, and synoptic storm events. Thus, we can assume that annual precipitation at Summit is substantially affected by the frequency of synoptic-scale cyclones, which can deliver precipitation to this high-altitude site. Koyama et al. (2017) documented that distinct changes in the frequency of winter Arctic cyclones (December through February) are not observed in the post-satellite era. Thus, the difference between our results and other estimates is likely to be related to Arctic cyclone activities in the warm season. While ASRv1 provides a good perspective on extreme cyclones, the ability to capture mesoscale high-latitude cyclones is still limited (e.g., Tilinina et al., 2014). Also, the precipitation microphysics and its parameterization cannot be expected to reproduce sub-grid scale precipitation processes. It is plausible to assume that annual POSS precipitation values evaluated here are reasonable as well as the values estimated by pits or regional climate models.

The results suggest that the phase of the NAO locally influence precipitation over Greenland and the surrounding waters. Thus, we need to pay attention to the geographical conditions. Where negative correlation coefficients appear, NW, BB, and AB, precipitation tends to decrease along with the increasing NAO index (Figs. 6 and 7). When NAO is positive, the greater pressure gradient between the subpolar low and the subtropical high can induce stronger westerlies, with speeds 8 m/s greater during high NAO winters than low NAO winters and anomalous northerly flow occurs across western Greenland (Hurrell, 1995). Consequently, the southwesterly flow that brings moisture to Greenland is weakened and results in a reduction of precipitation. Box et al. (2012), Fettweis et al. (2013), and Hanna et al. (2014) discussed the potential linkage between the negative NAO phase and precipitation amount in a different manner. Negative NAO indexes can induce an anticyclonic circulation or a blocking high system over Greenland, which can enhance southerly warm air advection. On the other hand, regions on the east side of Greenland: NE, SE, GS, and NA, show positive correlation coefficients (Figs. 6 and 7); precipitation over those regions tends to increase along with the increasing NAO index. When the NAO is in a positive phase, the Arctic Front occurring along the southeastern Greenland coast is possibly enhanced by the Icelandic Low, which can lead to increased pre-frontal rainfall over eastern coastal Greenland. Crawford and Serreze (2016) calculated the maximum Eady growth rate (EGR) which indicates the potential for cyclogenesis using the National Aeronautics and Space Administration's (NASA) Modern-Era Retrospective Analysis for Research and Applications (MERRA; Rienecker et al., 2011). Their results showed larger values over the southeastern coastal area of Greenland on average EGR map for winter (December–February). This implies that the corresponding coastal area is favorable for cyclonic activity and precipitation eventually. Almost no correlations appear over the rest of the regions, SW, DS, and LS between monthly precipitation and the NAO index. Sodemann et al. (2008) applied a Lagrangian method to the ERA-40

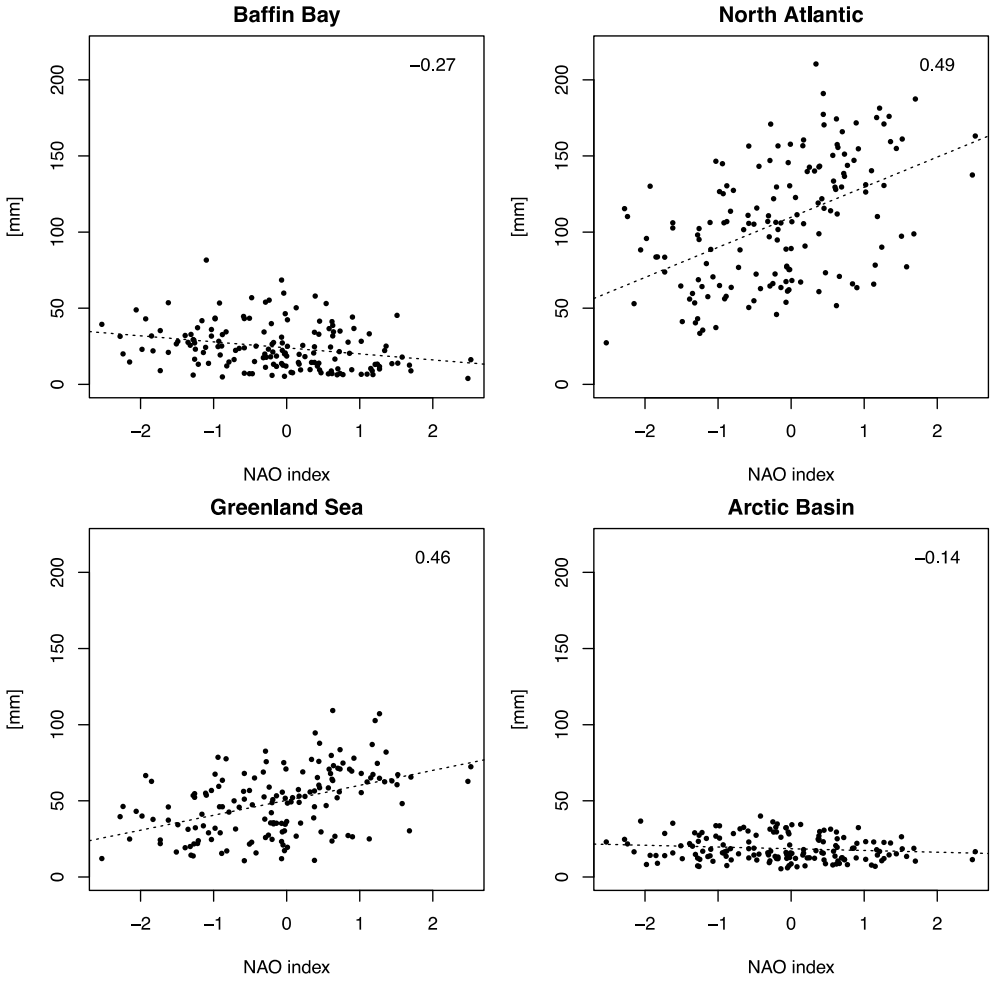

Fig. 7. Same as Fig. 6, but for four regions of the surrounding waters.

reanalysis and showed that the North Atlantic and Nordic Seas are moisture sources for Greenland precipitation. They found that the location of the identified moisture sources strongly varied with the NAO phase. Calder et al. (2008) studied a relationship between Greenland ice core-derived accumulation and NAO, and identified the linear accumulation-NAO relationship is stronger in western Greenland. Wong et al. (2015) confirmed that recent (1981–2012) changes in northwest Greenland annual precipitation are likely a response to a weakening NAO. Note that the ASRv1 monthly precipitation amount in the inland GrIS is still subject to errors as the results at Summit show. Validation of precipitation using gauge is not possible over the surrounding waters in parallel. Therefore, further investigation is preferable to discuss how the NAO phase affects precipitation over Greenland the extended area. A possible approach is utilizing measurements by the Millimeter-wave Cloud Radar (MMCR) at Summit, one of the ICECAPS instruments in addition to conventional estimation using data from snow pits.

5. Summary

In this study, monthly ASRv1 precipitation was compared with bias-corrected DMI precipitation around coastal Greenland and precipitation retrieved from POSS at Summit. While three different spatially averaged ASRv1 values are compared to the DMI precipitation to evaluate the spatial representativeness of the individual ASR grid point, the differences in the correlation coefficients between modeled data and observations for the different spatial averaging was found to be negligible (Table 2). Thus, ASRv1 precipitation data at the nearest grid point to the stations were used for comparison. The ASRv1 and DMI precipitation on the east and south side of Greenland showed good agreement, but uncertainty at Ikerasassuaq, the station nearest to Cape Farewell, South Greenland, in both datasets, appears to be larger (Fig. 2). The ASRv1 precipitation at Nuuk, the capital city of Greenland on the west coast of Greenland on the shore of the Labrador Sea, showed a negative bias when the observations exceeded 100 mm per month. One of the suspected causes is that local wind events account for the differences between the reanalysis and gauge data there. Even allowing for the reflectivity uncertainty of the POSS, which is a Doppler radar, the ASRv1 precipitation is overestimated at Summit, a high-elevation and inland research station (Fig. 2). While no independent precipitation gauges exist there, it is advisable to have further observations for comparison to confirm the ASRv1 overestimation.

The time series of precipitation illustrate pronounced high-frequency variability: each monthly precipitation value from both observed and modeled data is often beyond the 95% confidence intervals of the local polynomial regression fitting (Fig. 3). The ASRv1 fitted local polynomial regression of the southern stations show similar trends to each other as well as trends from the northeastern stations. It can be assumed that the similarity is coming from the numerical model's reproduction of synoptic-scale circulation effects on precipitation. However, the DMI regression results do not show similar trends among the stations and this suggests that local effects on precipitation, including several types of wind events and/or orographic effects, can surpass synoptic-scale circulation patterns in the observations and that these local effects are not captured in the ASRv1 data.

The relationship between the NAO index and ASRv1 precipitation over Greenland and surrounding waters is explored for different

geographical areas of Greenland (split into four regions based on the major ice sheet topographical divides in this study) and the surrounding waters (Figs. 5–7). The NAO index is moderately related to precipitation amount over northern Greenland, the North Atlantic, and Greenland Sea, where the magnitude of the correlation coefficients are between 0.32 and 0.49. Since the NAO is associated with changes in the surface westerlies across the North Atlantic and into Europe (Hurrell, 1995), moisture from the Labrador Sea can also vary along with NAO phases. However, the large and cold Greenland plateau can cause distinct local wind events originating from different mechanisms, such as westerly and easterly tip jets, barrier winds, katabatic wind, and cyclones that can significantly affect precipitation amount and its spatial distribution. While it is feasible to have a low correlation depending on the geographical effects, further study is necessary to understand the relationship.

Overall, the ASRv1 precipitation agrees with the corrected DMI gauge-based precipitation measured at coastal or near-coastal stations in Greenland, but the corresponding data at Ikerasassuaq and Nuuk are not the case. The ASRv1 precipitation at Summit, i.e., in a higher continental environment, is overestimated compared with the POSS observations. While similar variability is not found in the ASRv1 and DMI precipitation, the limited study period is not adequate for a detailed discussion. The NAO index and ASRv1 precipitation show moderate correlation over northern Greenland, the North Atlantic, and Greenland Sea. It is suspected that local wind events have a larger influence on precipitation where smaller correlation coefficients appear. Suggested future work to understand the discrepancies between the ASRv1 and DMI precipitation in Greenland coastal regions is to study various local wind events and the associated precipitation variations utilizing in-situ measurements during both strong positive and negative NAO phases. At high-altitude and inland areas, further observations are needed to confirm the ASRv1 overestimation.

Acknowledgments

This study was supported by National Science Foundation grants PLR-1304807. The ASRv1 forecast precipitation data have been produced by the Polar Meteorology Group/Byrd Polar and Climate Research Center/The Ohio State University and available at Research Data Archive at the National Center for Atmospheric Research, Computational and Information Systems Laboratory website. The POSS data and corrected DMI precipitation data were kindly provided by Matthew D. Shupe from Cooperative Institute for Research in Environmental Science, University of Colorado, and NOAA/Earth System Research Laboratory and Arno Hammann from Rutgers University, respectively. Elizabeth Cassano, John Cassano, and David Bromwich are acknowledged for providing helpful advice and comments on the draft manuscript.

Appendix A. Supplementary data

Supplementary data related to this article can be found at https://doi.org/10.1016/j.polar.2018.09.001.

References

Abe, M., Nozawa, T., Ogura, T., Takata, K., 2016. Effect of retreating sea ice on arctic cloud cover in simulated recent global warming. Atmos. Chem. Phys. 16, 14343–14356. https://doi.org/10.5194/acp-16-14343-2016.

Aðalgeirsdóttir, G., Stendel, M., Christensen, J.H., Cappelen, J., Vejen, F., Kjær, H.A., Mottram, R., Lucas-Picher, P., 2009. Assessment of the Temperature, Precipitation and Snow in the RCM HIRHAM4 at 25 Km Resolution, Danish Climate Centre Report 09-08. 80pp.

Akperov, M., Mokhov, I., Rinke, A., Dethloff, K., Matthes, H., 2015. Cyclones and their possible changes in the Arctic by the end of the twenty first century from regional climate model simulations. Theor. Appl. Climatol. 122, 85–96. https://doi.org/10.1007/s00704-014-1272-2.

Appenzeller, C., Schwander, J., Sommer, S., Stocker, T.F., 1998. The North Atlantic Oscillation and its imprint on precipitation and ice accumulation in Greenland. Geophys. Res. Lett. 25, 1939–1942. https://doi.org/10.1029/98GL01227.

Bales, R.C., McConnell, J.R., Mosley-Thompson, E., Csatho, B., 2001. Accumulation over the Greenland ice sheet from historical and recent records. J. Geophys. Res. Atmos. 106, 33813–33825. https://doi.org/10.1029/2001JD900153.

Bengtsson, L., Hodges, K.I., Roeckner, E., 2006. Storm tracks and climate change. J. Clim. 19, 3518–3543. https://doi.org/10.1175/JCLI3815.1.

Bengtsson, L., Hodges, K.I., Keenlyside, N., 2009. Will extratropical storms intensify in a warmer climate? J. Clim. 22, 2276–2301. https://doi.org/10.1175/2008JCLI2678.1.

Berkelhammer, M., Noone, D.C., Steen-Larsen, H.C., Bailey, A., Cox, C.J., ONeill, M.S., Schneider, D., Steffen, K., White, J.W.C., 2016. Surface-atmosphere decoupling limits accumulation at Summit, Greenland. Sci. Adv. 2https://doi.org/10.1126/sciadv.1501704. e1501704–e1501704.

Bintanja, R., Selten, F.M., 2014. Future increases in Arctic precipitation linked to local evaporation and sea-ice retreat. Nature 509, 479–482. https://doi.org/10.1038/nature13259.

Bougamont, M., Bamber, J.L., Greuell, W., 2005. A surface mass balance model for the Greenland Ice Sheet. J. Geophys. Res. Earth Surf. 110. https://doi.org/10.1029/2005JF000348.

Box, J.E., Fettweis, X., Stroeve, J.C., Tedesco, M., Hall, D.K., Steffen, K., 2012. Greenland ice sheet albedo feedback: thermodynamics and atmospheric drivers. Cryosphere 6, 821–839. https://doi.org/10.5194/tc-6-821-2012.

Bromwich, D.H., Chen, Q., Li, Y., Cullather, R.I., 1999. Precipitation over Greenland and its relation to the north atlantic oscillation. J. Geophys. Res. 104, 103–115. https://doi.org/10.1029/1999JD900373.

Bromwich, D., Kuo, Y.-H., Serreze, M., Walsh, J., Bai, L.-S., Barlage, M., Hines, K., Slater, A., 2010. Arctic system reanalysis: call for community involvement, eos. Trans. Am. Geophys. Union 91, 13. https://doi.org/10.1029/2010EO020001.

Bromwich, D.H., Wilson, A.B., Bai, L.-S., Moore, G.W.K., Bauer, P., 2016. A comparison of the regional arctic system reanalysis and the global ERA-interim reanalysis for the arctic. Q. J. R. Meteorol. Soc. 142, 644–658. https://doi.org/10.1002/qj.2527.

Calder, C.A., Craigmile, P.F., Mosley-Thompson, E., 2008. Spatial variation in the influence of the north atlantic oscillation on precipitation across Greenland. J. Geophys. Res. 113https://doi.org/10.1029/2007JD009227. D06112.

Cappelen, J., 2014. Weather Observations from Greenland 1958-2013 - Observation Data with Description. pp. 24 Technical Report 14-08.

Castellani, B.B., Shupe, M.D., Hudak, D.R., Sheppard, B.E., 2015. The annual cycle of snowfall at Summit, Greenland. J. Geophys. Res. Atmos. 120, 6654–6668. https://doi.org/10.1002/2015JD023072.

Chen, Q., Bromwich, D.H., Bai, L., 1997. Precipitation over Greenland retrieved by a dynamic method and its relation to cyclonic activity. J. Clim. 10, 839–870. https://doi.org/10.1175/1520-0442(1997)010<0839:POGRBA>2.0.CO;2.

Cohen, J.L., Furtado, C.J., Barlow, M.A., Alexeev, V.A., Cherry, J.E., 2012. Arctic warming, increasing snow cover and widespread boreal winter cooling. Environ. Res. Lett. 7, 14007. https://doi.org/10.1088/1748-9326/7/1/014007.

Crawford, A.D., Serreze, M.C., 2016. Does the summer arctic frontal zone influence Arctic Ocean cyclone activity? J. Clim. 29, 4977–4993. https://doi.org/10.1175/JCLI-D-15-0755.1.

Dee, D.P., Uppala, S.M., Simmons, A.J., Berrisford, P., Poli, P., Kobayashi, S., Andrae, U., Balmaseda, M.A., Balsamo, G., Bauer, P., Bechtold, P., Beljaars, A.C., van de Berg, L., Bidlot, J., Bormann, N., Delsol, C., Dragani, R., Fuentes, M., Geer, A.J., Haimberger, L., Healy, S.B., Hersbach, H., Hólm, E.V., Isaksen, L., Kållberg, P., Köhler, M., Matricardi, M., McNally, A.P., Monge-Sanz, B.M., Morcrette, J., Park, B., Peubey, C., de Rosnay, P., Tavolato, C., Thépaut, J., Vitart, F., 2011. The ERA-Interim reanalysis: configuration and performance of the data assimilation system. Q. J. R. Meteorol. Soc. 137, 553–597. https://doi.org/10.1002/qj.828.

Enderlin, E.M., Howat, I.M., Jeong, S., Noh, M.-J., van Angelen, J.H., van den Broeke, M.R., 2014. An improved mass budget for the Greenland ice sheet. Geophys. Res. Lett. 41, 866–872. https://doi.org/10.1002/2013GL059010.

Ettema, J., van den Broeke, M.R., van Meijgaard, E., van de Berg, W.J., Bamber, J.L., Box, J.E., Bales, R.C., 2009. Higher surface mass balance of the Greenland ice sheet revealed by high-resolution climate modeling. Geophys. Res. Lett., L12501. https://doi.org/10.1029/2009GL038110.

Fettweis, X., Hanna, E., Lang, C., Belleflamme, A., Erpicum, M., Gallée, H., 2013. Brief communication "Important role of the mid-tropospheric atmospheric circulation in the recent surface melt increase over the Greenland ice sheet". Cryosphere 7, 241–248. https://doi.org/10.5194/tc-7-241-2013.

Fettweis, X., Box, J.E., Agosta, C., Amory, C., Kittel, C., Lang, C., van As, D., Machguth, H., Gallée, H., 2017. Reconstructions of the 1900–2015 Greenland ice sheet surface mass balance using the regional climate MAR model. Cryosphere 11, 1015–1033. https://doi.org/10.5194/tc-11-1015-2017.

Fitzgerald, P.W., Bamber, J.L., Ridley, J.K., Rougier, J.C., 2012. Exploration of parametric uncertainty in a surface mass balance model applied to the Greenland ice sheet. J. Geophys. Res. Earth Surf. 117. https://doi.org/10.1029/2011JF002067.

Fonseca, R.M., Zhang, T., Yong, K.-T., 2015. Improved simulation of precipitation in the tropics using a modified BMJ scheme in the WRF model. Geosci. Model Dev. (GMD) 8, 2915–2928. https://doi.org/10.5194/gmd-8-2915-2015.

Forsberg, R., Sørensen, L., Simonsen, S., 2017. Greenland and Antarctica ice sheet mass changes and effects on global sea level. Surv. Geophys. 38, 89–104. https://doi.org/10.1007/s10712-016-9398-7.

Francis, J.A., Chan, W., Leathers, D.J., Miller, J.R., Veron, D.E., 2009. Winter Northern Hemisphere weather patterns remember summer Arctic sea-ice extent. Geophys. Res. Lett. 36. https://doi.org/10.1029/2009GL037274.

Ghatak, D., Deser, C., Frei, A., Gong, G., Phillips, A., Robinson, D.A., Stroeve, J., 2012. Simulated Siberian snow cover response to observed Arctic sea ice loss, 1979-2008. J. Geophys. Res. Atmos. 117. https://doi.org/10.1029/2012JD018047.

Hanna, E., Fettweis, X., Mernild, S.H., Cappelen, J., Ribergaard, M.H., Shuman, C.A., et al., 2014. Atmospheric and oceanic climate forcing of the exceptional Greenland ice sheet surface melt in summer 2012. Int. J. Climatol. 34, 1022–1037. https://doi.org/10.1002/joc.3743.

Hurrell, J.W., 1995. Decadal trends in the north Atlantic oscillation: regional

temperatures and precipitation. Science 269, 676–679. https://doi.org/10.1126/science.269.5224.676.
Inoue, J., Hori, M.E., Takaya, K., 2012. The role of Barents sea ice in the wintertime cyclone track and emergence of a warm-Arctic cold-Siberian anomaly. J. Clim. 25, 2561–2568. https://doi.org/10.1175/JCLI-D-11-00449.1.
Jahn, A., Kay, J.E., Holland, M.M., Hall, D.M., 2016. How predictable is the timing of a summer ice-free Arctic? Geophys. Res. Lett. 43, 9113–9120. https://doi.org/10.1002/2016GL070067.
Jones, P.D., Jonsson, T., Wheeler, D., 1997. Extension to the North Atlantic oscillation using early instrumental pressure observations from Gibraltar and south-west Iceland. Int. J. Climatol. 17, 1433–1450.
Kattsov, V.M., Walsh, J.E., Chapman, W.L., Govorkova, V.A., Pavlova, T.V., Zhang, X., 2007. Simulation and projection of arctic freshwater budget components by the IPCC AR4 global climate models. J. Hydrometeorol. 8, 571–589. https://doi.org/10.1175/JHM575.1.
Kay, J.E., Gettelman, A., 2009. Cloud influence on and response to seasonal Arctic sea ice loss. J. Geophys. Res. 114, D18204. https://doi.org/10.1029/2009JD011773.
Koerner, R., Russell, R.D., 1979. $\delta^{18}O$ variations in snow on the Devon Island ice cap, Northwest Territories, Canada. Can. J. Earth Sci. 16, 1419–1427. https://doi.org/10.1139/e79-126.
Kopec, B.G., Feng, X., Michel, F.A., Posmentier, E.S., 2016. Influence of sea ice on Arctic precipitation. Proc. Natl. Acad. Sci. Unit. States Am. 113, 46–51. https://doi.org/10.1073/pnas.1504633113.
Koyama, T., Stroeve, J., Cassano, J., Crawford, A., 2017. Sea ice loss and Arctic cyclone activity from 1979 to 2014. J. Clim. 30https://doi.org/10.1175/JCLI-D-16-0542.1. JCLI-D-16-0542.1.
Langen, P.L., Fausto, R.S., Vandecrux, B., Mottram, R.H., Box, J.E., 2017. Liquid water flow and retention on the Greenland Ice Sheet in the regional climate model HIRHAM5: local and large-scale impacts. Front. Earth Sci. 4, 110. https://doi.org/10.3389/feart.2016.00110.
Lim, Y.-K., Schubert, S.D., Nowicki, S.M.J., Lee, J.N., Molod, A.M., Cullather, R.I., Zhao, B., Velicogna, I., 2016. Atmospheric summer teleconnections and Greenland Ice Sheet surface mass variations: insights from MERRA-2. Environ. Res. Lett. 11, 24002. https://doi.org/10.1088/1748-9326/11/2/024002.
Liston, G.E., Sturm, M., 2004. The role of winter sublimation in the Arctic moisture budget, Nord. Hydrol. 35, 325–334.
Liu, J., Curry, J.A., Wang, H., Song, M., Horton, R.M., 2012. Impact of declining Arctic sea ice on winter snowfall. Proc. Natl. Acad. Sci. Unit. States Am. 109, 4074–4079. https://doi.org/10.1073/pnas.1114910109.
Massonnet, F., Fichefet, T., Goosse, H., Bitz, C.M., Philippon-Berthier, G., Holland, M.M., Barriat, P.-Y., 2012. Constraining projections of summer Arctic sea ice. Cryosphere 6, 1383–1394. https://doi.org/10.5194/tc-6-1383-2012.
Matrosov, S.Y., 2007. Modeling backscatter properties of snowfall at millimeter wavelengths. J. Atmos. Sci. 64, 1727–1736. https://doi.org/10.1175/JAS3904.1.
Matrosov, S.Y., Campbell, C., Kingsmill, D., Sukovich, E., 2009. Assessing snowfall rates from X-band radar reflectivity measurements. J. Atmos. Ocean. Technol. 26, 2324–2339. https://doi.org/10.1175/2009JTECHA1238.1.
McCabe, G.J., Clark, M.P., Serreze, M.C., 2001. Trends in northern Hemisphere surface cyclone frequency and intensity. J. Clim. 14, 2763–2768. https://doi.org/10.1175/1520-0442(2001)014<2763:TINHSC>2.0.CO;2.
Mekis, E., Hogg, W.D., 1999. Rehabilitation and analysis of Canadian daily precipitation time series. Atmos.-Ocean 37, 53–85. https://doi.org/10.1080/07055900.1999.9649621.
Mernild, S.H., Hanna, E., McConnell, J.R., Sigl, M., Beckerman, A.P., Yde, J.C., Cappelen, J., Malmros, J.K., Steffen, K., 2015. Greenland precipitation trends in a long-term instrumental climate context (1890-2012): evaluation of coastal and ice core records. Int. J. Climatol. 35, 303–320. https://doi.org/10.1002/joc.3986.
Mishchenko, M.I., 2000. Calculation of the amplitude matrix for a nonspherical particle in a fixed orientation. Appl. Optic. 39, 1026. https://doi.org/10.1364/AO.39.001026.
Moore, G.W.K., Renfrew, I.A., 2005. Tip jets and barrier winds: a QuikSCAT climatology of high wind speed events around Greenland. J. Clim. 18, 3713–3725. https://doi.org/10.1175/JCLI3455.1.
Moore, G.W.K., Bromwich, D.H., Wilson, A.B., Renfrew, I., Bai, L., 2016. Arctic System Reanalysis improvements in topographically forced winds near Greenland. Q. J. R. Meteorol. Soc. 142, 2033–2045. https://doi.org/10.1002/qj.2798.
Mosley-Thompson, E., Readinger, C.R., Craigmile, P., Thompson, L.G., Calder, C.A., 2005. Regional sensitivity of Greenland precipitation to NAO variability. Geophys. Res. Lett. 32, L24707. https://doi.org/10.1029/2005GL024776.
Niwano, M., Aoki, T., Hashimoto, A., Matoba, S., Yamaguchi, S., Tanikawa, T., Fujita, K., Tsushima, A., Iizuka, Y., Shimada, R., Hori, M., 2018. NHM–SMAP: spatially and temporally high-resolution nonhydrostatic atmospheric model coupled with detailed snow process model for Greenland Ice Sheet. Cryosphere 12, 635–655. https://doi.org/10.5194/tc-12-635-2018.
Noël, B., van de Berg, W.J., van Meijgaard, E., Kuipers Munneke, P., van de Wal, R.S.W., van den Broeke, M.R., 2015. Evaluation of the updated regional climate model RACMO2.3: summer snowfall impact on the Greenland Ice Sheet. Cryosphere 9, 1831–1844. https://doi.org/10.5194/tc-9-1831-2015.
Notz, D., Stroeve, J., 2016. Observed Arctic sea-ice loss directly follows anthropogenic CO 2 emission. Science 354, 747–750. https://doi.org/10.1126/science.aag2345.
Orsolini, Y.J., Senan, R., Balsamo, G., Doblas-Reyes, F.J., Vitart, F., Weisheimer, A., Carrasco, A., Benestad, R.E., 2013. Impact of snow initialization on sub-seasonal forecasts. Clim. Dynam. 41, 1969–1982. https://doi.org/10.1007/s00382-013-1782-0.
Peterson, T.C., Vose, R.S., 1997. An overview of the global historical climatology network temperature database. Bull. Am. Meteorol. Soc. 78, 2837–2849.
Rasmussen, R., et al., 2012. How well are we measuring snow: the NOAA/FAA/NCAR winter precipitation test bed. Bull. Am. Meteorol. Soc. 93, 811–829. https://doi.org/10.1175/BAMS-D-11-00052.1.
Rienecker, M.M., Suarez, M.J., Gelaro, R., Todling, R., Liu, J. BacmeisterE., Bosilovich, M.G., Schubert, S.D., Takacs, L., Kim, G., Bloom, S., Chen, J., Collins, D., Conaty, A., da Silva, A., Gu, W., Joiner, J., Koster, R.D., Lucchesi, R., Molod, A., Owens, T., Pawson, S., Pegion, P., Redder, C.R., Reichle, R., Robertson, F.R., Ruddick, A.G., Sienkiewicz, M., Woollen, J., 2011. MERRA: NASA's Modern-Era retrospective analysis for research and Applications. J. Clim. 24, 3624–3648. https://doi.org/10.1175/JCLI-D-11-00015.1.
Rogers, J.C., 1984. The association between the north atlantic oscillation and the southern oscillation in the Northern Hemisphere. Mon. Weather Rev. 112 1999–2015.
Screen, J.A., Simmonds, I., 2010. The central role of diminishing sea ice in recent Arctic temperature amplification. Nature 464, 1334–1337. https://doi.org/10.1038/nature09051.
Screen, J.A., Simmonds, I., Deser, C., Tomas, R., 2013. The atmospheric response to three decades of observed Arctic sea ice loss. J. Clim. 26, 1230–1248. https://doi.org/10.1175/JCLI-D-12-00063.1.
Serreze, M.C., Barrett, A.P., Stroeve, J.C., Kindig, D.N., Holland, M.M., 2009. The emergence of surface-based Arctic amplification. Cryosphere 3, 11–19. https://doi.org/10.5194/tc-3-11-2009.
Serreze, M.C., Barrett, A.P., Stroeve, J., 2012. Recent changes in tropospheric water vapor over the Arctic as assessed from radiosondes and atmospheric reanalyses. J. Geophys. Res. Atmos. 117. https://doi.org/10.1029/2011JD017421.
Serreze, M.C., Barry, R.G., 2014. The Arctic Climate System. Cambridge University Press, Cambridge. https://doi.org/10.1017/CBO9781139583817.
Serreze, M.C., Crawford, A.D., Barrett, A.P., 2015. Extreme daily precipitation events at spitsbergen, an arctic island. Int. J. Climatol. 35, 4574–4588. https://doi.org/10.1002/joc.4308.
Serreze, M.C., Stroeve, J., 2015. Arctic sea ice trends, variability and implications for seasonal ice forecasting. Philos. Trans. R. Soc. A Math. Phys. Eng. Sci. 373, 20140159. https://doi.org/10.1098/rsta.2014.0159.
Shepherd, A., et al., 2012. A reconciled estimate of ice-sheet mass balance. Science 338, 1183–1189. https://doi.org/10.1126/science.1228102.
Sheppard, B.E., Joe, P.I., 2008. Performance of the precipitation occurrence sensor system as a precipitation gauge. J. Atmos. Ocean. Technol. 25, 196–212. https://doi.org/10.1175/2007JTECHA957.1.
Sodemann, H., Schwierz, C., Wernli, H., 2008. Interannual variability of Greenland winter precipitation sources: Lagrangian moisture diagnostic and North Atlantic Oscillation influence. J. Geophys. Res. 113, D03107. https://doi.org/10.1029/2007JD008503.
Stroeve, J., 2001. Assessment of Greenland albedo variability from the advanced very high resolution radiometer Polar Pathfinder data set. J. Geophys. Res. Atmos. 106, 33989–34006. https://doi.org/10.1029/2001JD900072.
Stroeve, J.C., Kattsov, V., Barrett, A., Serreze, M., Pavlova, T., Holland, M., Meier, W.N., 2012a. Trends in Arctic sea ice extent from CMIP5, CMIP3 and observations. Geophys. Res. Lett. 39. https://doi.org/10.1029/2012GL052676.
Stroeve, J.C., Serreze, M.C., Holland, M.M., Kay, J.E., Malanik, J., Barrett, A.P., 2012b. The Arctic's rapidly shrinking sea ice cover: a research synthesis. Climatic Change 110, 1005–1027. https://doi.org/10.1007/s10584-011-0101-1.
Stroeve, J., Notz, D., 2015. Insights on past and future sea-ice evolution from combining observations and models. Global Planet. Change 135, 119–132. https://doi.org/10.1016/j.gloplacha.2015.10.011.
Stroeve, J.C., Mioduszewski, J.R., Rennermalm, A., Boisvert, L.N., Tedesco, M., Robinson, D., 2017. Investigating the local scale influence of sea ice on Greenland surface melt. Cryosphere Discuss. 1–36. https://doi.org/10.5194/tc-2017-65.
Tedesco, M., Fettweis, X., van den Broeke, M.R., van de Wal, R.S.W., Smeets, C.J.P.P., van de Berg, W.J., Serreze, M.C., Box, J.E., 2011. The role of albedo and accumulation in the 2010 melting record in Greenland. Environ. Res. Lett. 6, 14005. https://doi.org/10.1088/1748-9326/6/1/014005.
Tilinina, N., Gulev, S.K., Bromwich, D.H., 2014. New view of Arctic cyclone activity from the Arctic system reanalysis. Geophys. Res. Lett. 41, 1766–1772. htpps://doi:10.1002/ 2013GL058924.
Ulbrich, U., Leckebusch, G.C., Pinto, J.G., 2009. Extra-tropical cyclones in the present and future climate: a review. Theor. Appl. Climatol. 96, 117–131. https://doi.org/10.1007/s00704-008-0083-8.
Vazquez, M., Nieto, R., Drumond, A., Gimeno, L., 2017. Extreme sea ice loss over the arctic: an analysis based on anomalous moisture transport. Atmosphere 8, 32. https://doi.org/10.3390/atmos8020032.
Vihma, T., 2014. Effects of Arctic sea ice decline on weather and climate: a review. Surv. Geophys. 35, 1175–1214. https://doi.org/10.1007/s10712-014-9284-0.
Vizcaíno, M., Lipscomb, W.H., Sacks, W.J., van den Broeke, M., 2014. Greenland surface mass balance as simulated by the community earth system model. Part II: twenty-first-century changes. J. Clim. 27, 215–226. https://doi.org/10.1175/JCLI-D-12-00588.1.
Wong, G.J., Osterberg, E.C., Hawley, R.L., Courville, Z.R., Ferris, D.G., Howley, J.A., 2015. Coast-to-interior gradient in recent northwest Greenland precipitation trends (1952–2012). Environ. Res. Lett. 10, 114008. https://doi.org/10.1088/1748-9326/10/11/114008.
Yang, D., Ishida, S., Goodison, B.E., Gunther, T., 1999. Bias correction of daily precipitation measurements for Greenland. J. Geophys. Res. 104, 6171. https://doi.org/10.1029/1998JD200110.
Yin, J.H., 2005. A consistent poleward shift of the storm tracks in simulations of 21st century climate. Geophys. Res. Lett. 32. https://doi.org/10.1029/2005GL023684.
Zhang, X., Walsh, J.E., Zhang, J., Bhatt, U.S., Ikeda, M., 2004. Climatology and interannual variability of Arctic cyclone activity: 1948-2002. J. Clim. 17https://doi.org/10.1175/1520-0442(2004)017<2300:CAIVOA>2.0.CO;2. 2300–2317.